0.5e- rms Read Noise CMOS Image Sensors and Sub-Electron Image Processing for Night Vision Application

Kwang Bo Cho and Brian Johnson
BAE Systems
kwangbo.cho@baesystems.com
1841 Zanker Road, Suite 50, San Jose, CA 95112 USA

***Abstract* - In this paper we present the 0.5e- root mean square (rms) read noise 9.5Mpixel 4K HWK4123 and 1.6Mpixel HWK1411 sensors realized with 65nm CMOS Image Sensor (CIS) technology. These sensors are suitable for very low-light imaging applications such as night vision. We show the sensor architecture and analog signal path used to achieve very low read noise, their performances and comparison, including showing the high near infrared quantum efficiency. Based on these sensors, we show Signal-to Noise Ratio (SNR) measurements and sub-electron images and video processing results.**

1. Introduction

There has been good progress made on image sensor process technology and development over the last several years to achieve low read noise, low dark current, and high quantum efficiency for surveillance, security, and night vision applications [1]. An example is our scientific Complementary Metal-Oxide Semiconductor (sCMOS) 65nm technology with Back Side Illumination (BSI) and improved Near-Infrared Quantum Efficiency (NIR QE). This extends the usable spectrum to 1100nm, delivers extreme low noise, reduces dark current, and boosts QE.

We developed the HWK4123 sensor based on this technology. Using the latest sCMOS BSI technology to enhance NIR QE by increasing the thickness of the epitaxial layer (epi) and applying deeper Deep Trench Isolation (DTI), we developed the HWK1411 to improve low light capability with a larger pixel and even higher NIR QE.

In the first part of this paper, we will present the HWK4123 and HWK1411 sensors, their architectures, measured performances and a comparison. In the second part of this paper, we will discuss recent low light image and video enhancements using these sensors, especially focusing on night vision applications.

2. Low Light Image Sensors – HWK4123 and HWK1411

The HWK4123 incorporates sCMOS BSI technology resulting in a very low-light capable sensor with 4.6µm x 4.6µm pixels, 4K (4108 x 2308) resolution with a market leading 0.5e- rms read noise at 120 Frames Per Second (FPS). In addition, the enhanced NIR QE process leverages the NIR content of nightglow for improved night vision, combining exceptionally low read noise with high quantum efficiency BSI processing enables starlight (<1mLux) imaging capability at 60FPS. The HWK4123 delivers the performance demanded by night vision and high-end surveillance applications with 4K resolution.

Also in the HWK family of products, the HWK1411 incorporates the latest sCMOS BSI technology with enhanced NIR QE into its design. With 1.6M 8µm pixels, this provides an ultra-low light image sensor capable of imaging down to overcast starlight (0.1mLux), meeting recent night vision performance requirements. The HWK1411 has 1440 x 1104 resolution with an 8µm x 8µm pixel and reaches 120FPS at full resolution. The uncompressed data width is 16 bits-per-pixel, which offers up to 96dB high dynamic range for the image. The 4-lane Mobile Industry Processor Interface (MIPI) at 1.5GHz is utilized to simplify integration with industrial ecosystems. It enables night vision applications with the benefits of reduced Size, Weight and Power (SWaP).

The HWK1411 low-light digital image sensor with on-chip 16-bit High Dynamic Range (HDR) processing and dark current compensation with frame memory is designed to capture imagery under overcast starlight (0.1mLux) conditions. It combines,

- Large photon-collection array with world-class high NIR quantum efficiency for light sensitivity.
- Ability to see small changes in contrast because of low read noise, 0.5e-, achieved by novel analog design.
- Reduced signal noise due to its low dark current (3e-/s @30C).

This HWK1411 enables the military night vision market's transition into the digital domain because the HWK1411 can replace larger and heavier legacy technology. It provides high-performance imaging capabilities in all light conditions. Its design is optimal for battery-powered systems, unmanned platforms, and intelligence, surveillance and reconnaissance applications. This SWaP optimized design creates a forward-looking design path to next-gen systems that offer technologies such as sensor fusion, augmented reality and artificial intelligence. Enabling these technologies transforms how warfighters perceive the battle space in ultra-low-light conditions.

Furthermore, HWK1411 is integrated into a compact Multi-Chip Module (MCM) with a microprocessor, flash memory, power management, a flexible cable for plug-and-play connectivity, and a high-performance glass lens for an optimal field of view.

2.1 Sensor Architecture

Figure 1 shows the HWK4123 and HWK1411 layouts with package. Both HWK4123 and HWK1411 have five-transistor (5T) pixels with pinned photodiodes and use a dual gain column amplifier architecture resulting in 16-bits per pixel to encompass the full HDR. Low-gain and high-gain signal paths provide analog to digital conversions at different gain factors on a pixel by pixel basis.

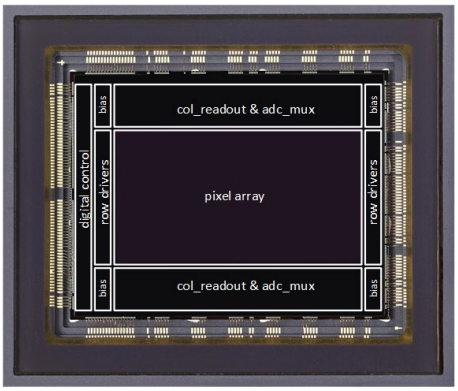

(a)HWK4123 Layout

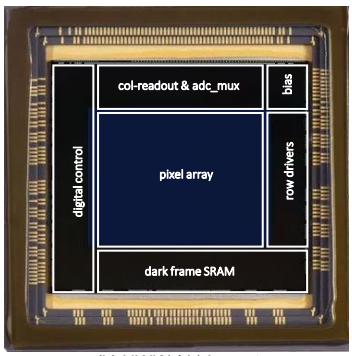

(b) HWK1411 Layout

Figure 1. HWK4123 and HWK1411 Layouts with Package.

Figure 2 shows the simplified analog signal path that includes the pixel, column amplifier, gain comparator, variable bandwidth buffer, sample and

hold capacitors, and Analog to Digital Convertor (ADC) module. The column amplifier has two gain modes: a high gain mode of up to 32x and a low gain mode of 1x. The gain comparator is used to automatically drop the gain to unity if the amplifier output exceeds vref_LG, an on-chip programmable reference voltage. The full well capacity is limited by the voltage swing at the floating diffusion node in low gain (1x) mode with a linear full well capacity of 7000e-. The column amplifier bandwidth was carefully adjusted such that the minimum thermal noise contribution from the amplifier is achieved in high gain mode. Further reduction of the bandwidth is available in the variable bandwidth stage. For operation at 120fps, the bandwidth can be set to obtain an average read noise of 0.5e- rms.

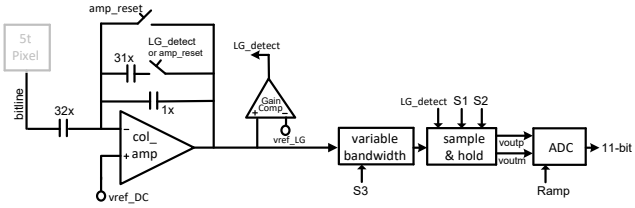

Figure 2. Simplified diagram of the analog signal path.

Figure 3 shows the HDR processing for high gain and low gain merging. By merging either the low-gain signal or the high-gain signal for each pixel with respect to a threshold signal level and post gain adjustment, we maintain both low noise performance at high-gain and large signal at low gain. The result is high native dynamic range in a frame. The HWK4123 merging process is implemented off-chip, while the HWK1411 performs the merging on-chip.

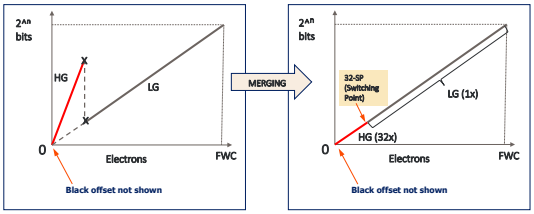

Figure 3. HDR processing for high gain and low gain merging.

2.2 Performance and Measurements

Table 1 shows the relative performance of the HWK4123 and the HWK1411. The key highlight is the 0.5e- rms read noise which enables imaging in darker scenarios. In addition, the enhanced NIR QE process leverages the existing nightglow for improved low-light imaging. By merging high gain (32x) and low gain (1x) outputs, either off-chip for the HWK4123 or on-chip for the HWK1411, they achieve 83dB linear dynamic range to show more detail in high contrast scenes. The pixel's low dark current also enables low noise at longer exposure times for night vision applications.

Table 1. HWK4123 and HWK1411 Performances and Comparison

Parameter	HWK4123	HWK1411
Resolution	9.5Mp (4108 x 2308)	1.6Mp (1440 x 1100)
Pixel (µm)	4.6	8.0
Conversion Gain (µV/e-)	170	170
Read Noise at 32x, 120FPS (e- rms)	0.5	0.5
Linear Full Well Capacity (e-)	7000	7000
Peak QE (%)	87	80
QE (850nm, %)	48	57
QE (940nm, %)	27	39
QE (1060nm, %)	2	6
High Dynamic Range (HDR) (dB)	83	83
Dark Current (e-/sec, at 30C)	2	3
Power Consumption at 120FPS (W)	1.8	0.55

Sensitivity in the NIR domain is key for numerous applications, such as low light, night vision, and biometrics (face recognition for access control, etc.). The major increase of QE in the NIR domain is by increasing the depth of the silicon photodiode pixels. The HWK4123 and HWK1411 have an epi thickness of 2.5 µm and 6.0µm epi respectively. Figure 4 shows their QE.

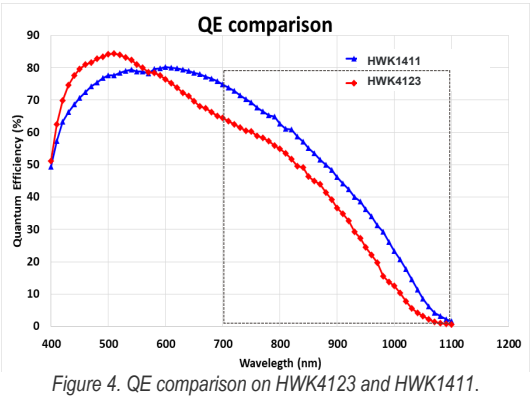

Figure 4. QE comparison on HWK4123 and HWK1411.

3. Test Setup and SNR Measurements

3.1 SNR1-NV Setup and Light Levels

SNR is a good measurement to determine image performance, usually this is done with a target reflectivity of 18% (Gray). The minimum acceptable SNR requirement for security and surveillance applications is typically 1 which occurs when the signal level equals the noise. The light level at which this occurs is referred to as the SNR1. For night vision applications, it is critical to detect objects even when the SNR is below 1. Here we define a new measurement, SNR Night Vision (SNR-NV), where some of the settings for SNR have been changed to better represent night vision applications. A comparison of the settings for SNR-NV and SNR are shown in Table 2 below. The light source for SNR-NV is 2800K to better simulate the spectrum of light from night-glow and the target reflectivity is increased to 95% to better model limits of visibility at very low light levels.

Table 2. SNR-NV and SNR Settings

Parameter	SNR-NV Setting	SNR Setting
Light Source	2800K	3200K
Exposure Time	1/60 second	1/60 second
Lens	F/1.4	F/1.4
IR Cut Filter	Not used	Used
Distance to target	1 Meter	1 Meter
Target Reflectivity	95% (White)	18% (Gray)

Figure 5(a) shows our SNR-NV test setup including the light source, target, light meter (PR-745) and test Image. The light source is an integrating sphere which is illuminated with a 2800K tungsten source. The target is the white patch of an Xrite color checker which has a Lambertian reflectivity of 95%.

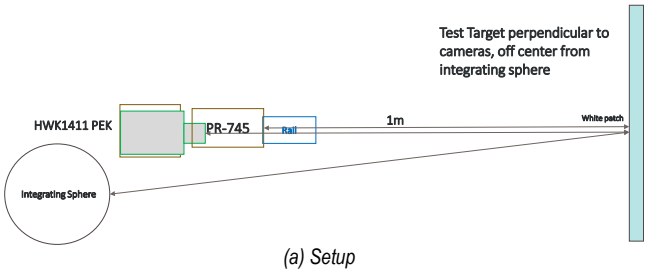

(a) Setup

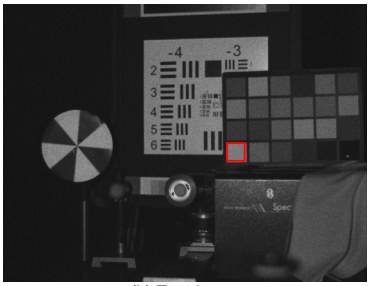

(b) Test Image

Figure 5. SNR-NV Setup and Test Image.

The Table 3 below helps provide an idea of the very low light levels required for night vision applications. We are generally interested in light levels less than 1mlux, which corresponds to a moonless clear night or less.

Table 3. Light Levels at Typical Conditions

Light Level	Condition
1,000.0mlux	Deep Twilight
100.0mlux	Full Moon on a clear night
10.0mlux	Quarter Moon
1.0mlux	Starlight on moonless clear night sky
0.1mlux	Overcast Starlight on moonless overcast night sky

3.2 SNR Measurements

Figure 6 shows the HWK4123 and HWK1411 SNR-NV measurements and comparison at 60FPS with respect to different light levels.

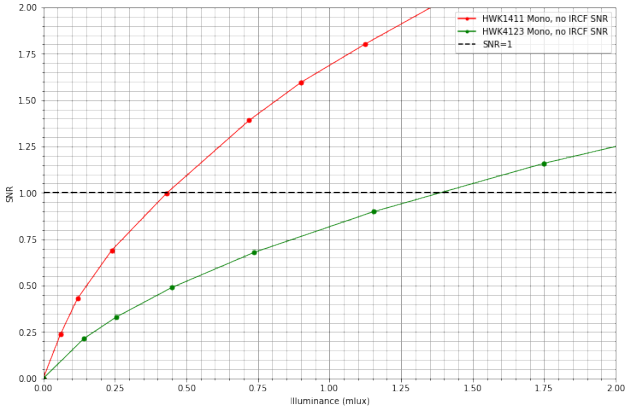

Figure 6. HWK4123 and HWK1411 SNR-NV measurements and comparison at 60FPS.

Figure 7 shows the SNR-NV vs mlux for the HWK1411 Monochrome sensor without an Infrared Cut Filter (IRCF), the HWK1411 Color sensor without IRCF and the HWK1411 Color sensor with IRCF.

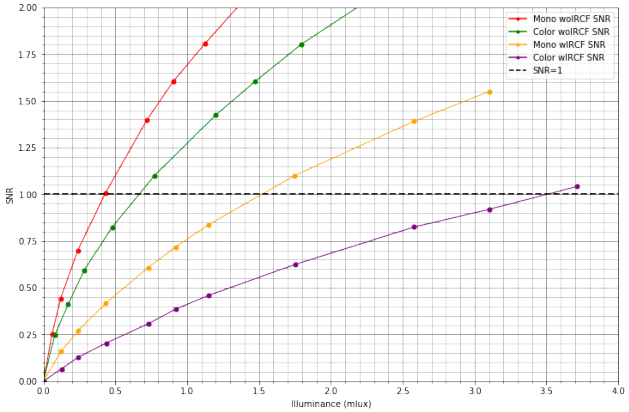

Figure 7. HWK1411 monochrome and color sensors SNR-NV measurement at 60FPS.

4. Low Light Image Processing for Night Vision Applications

In this section, we discuss video processing to improve the quality of low light images and the tradeoffs involved. Since the HWK1411 has better performance at low light, we will use HWK1411 to present improvements.

4.1 Low Light Performance Improvement

In order to get better image quality at the extreme light conditions such as starlight and overcast starlight, we need to increase signal response and reduce noise as much as we can.

To increase signal, first, we need to choose the larger pixel with given resolution and optical format, second, we need to improve QE including NIR, third, we can maximize integration time, increase sensor analog gain, slow frame rate and do pixel summing for signal or binning (averaging) for noise as long as we meet operational requirements. Note that we prefer pixel summing to binning (averaging) to get the bigger signal. Fourth, to increase the amount of light collected, we can choose lower F# lens.

To reduce noise, first, we need to reduce read noise as small as possible at the given gain and frame rate, second, we need to reduce dark current to reduce dark current shot noise. Third, we can apply post image/video processing to reduce the noise using filters like Bilateral, Binomial, Box, Gaussian, etc. Figure 8 shows image comparisons between a raw, unprocessed image and differently binned images.

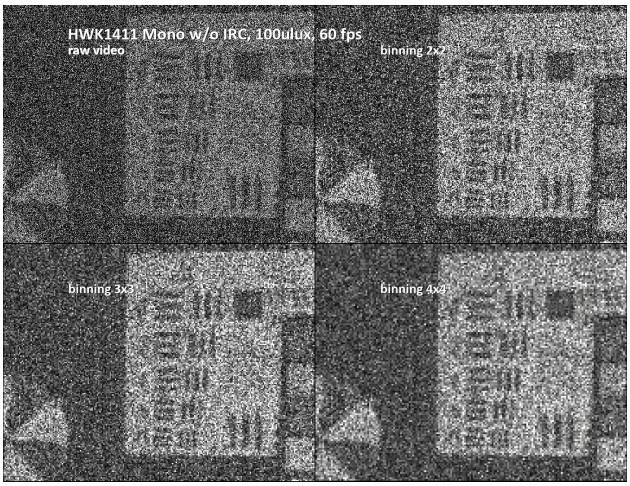

Figure 8. Comparison between raw and binned images.

Figure 9 shows image comparison between a raw image, a 3x3 binned image, a box filtered image and a Gaussian filtered image.

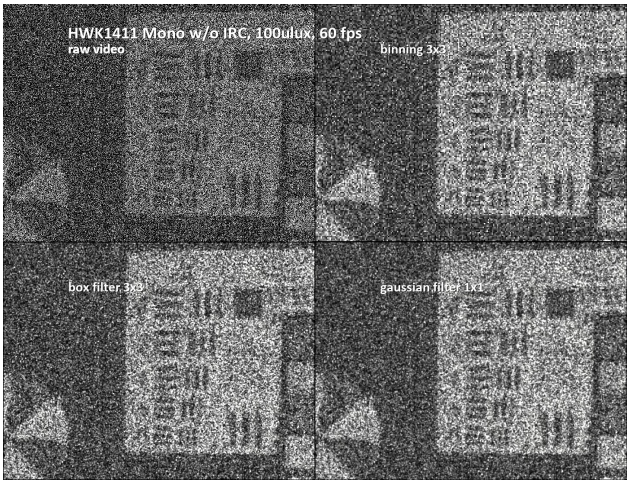

Figure 9. Raw, 3x3 binned, box filtered and Gaussian filtered images.

Table 4 shows the SNR-NV measurements of raw, 3x3 binned, box filtered, and Gaussian filtered images at 100µlux (overcast starlight) and 60FPS. In the raw image at 100µlux, we have less than 0.4e- average signal/pixel and a measured SNR-NV = 0.44. As we can see in Figure 9, we can still recognize object at this sub-electron image.

Table 4. SNR-NV measurement between raw image, 3x3 binning image, box filter and Gaussian filter image captures at 100µlux, 60FPS

At 100µLux Light Condition	SNR-NV
Raw	0.44
Binned	2.45
Box	2.99
Gaussian	4.04

4.2 Sub-Electron Image and Video Processing

An interesting area for study is the sub-electron image region where the photon shot noise is bigger than signal, meaning SNR is always less than 1. During the study, we notice that although we measure an SNR of less

than 1 in a still image, when watching video our eyes see much cleaner video due to our brain's visual processing filtering out the noise. Figure 10 shows a raw capture and averaged images at 100µlux. Based on subjective tests, most people feel that the image quality of an average of 9 frames, is close to the quality of the raw video. This means we perceive an SNR improvement of 3x due to our eye and visual cortex processing the video.

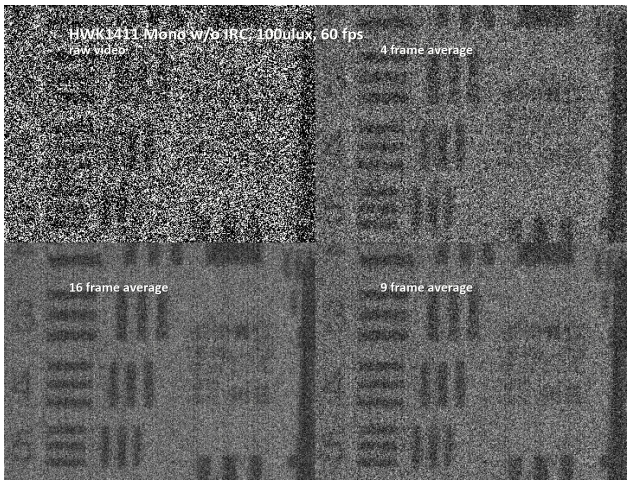

Figure 10. Experiment on raw video vs. averaging images.

This indicates our effective noise in video is 1/3 of measured noise in a still image, so our useful video signal range can be extended further down. Therefore, when we have a 1e- or sub-electron pixel image, even though it is less than SNR1, we may see an acceptable image and better video.

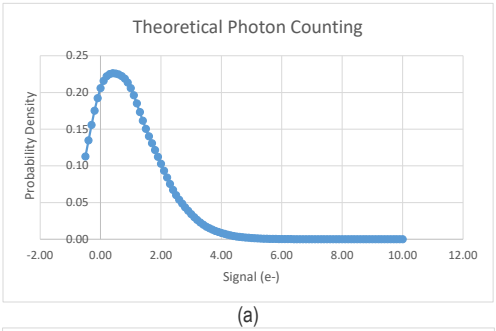

(a)

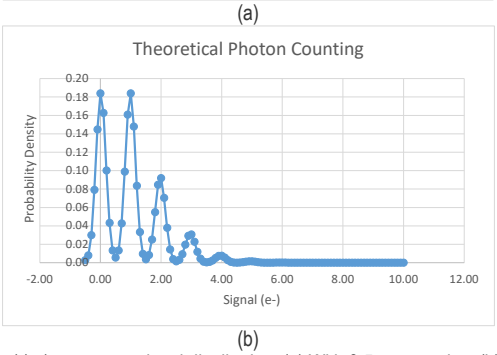

(b)

Figure 11. 1e- average signal distribution. (a) With 0.5e- rms noise. (b) With 0.17e- rms noise.

To check average 1e- signal on pixel and display on monitor, Liquid Crystal Display (LCD), Light Emitting Diode (LED) display, or Head Mounted Display (HMD) properly, we would like to know signal distribution. In Figure 11, we show two different signal distributions, (a) a 1e- average signal with 0.5e- rms noise and (b) a 1e- average signal with 0.17e- rms noise. At the 99th percentile, it will be a 4e- signal. A signal with an average 1e- per pixel can be as large as 4e- signal at each frame based on distribution.

Another constraint to consider is a limitation on Conversion Factor (CF). The HWK1411 has a CF of 8DN/e- (Data Numbers/electron), meaning 1 electron is represented by only 8DN. If we want to have more DN/e-, we will need to increase analog gain or ADC bit depth, or digital gain with missing bits.

In addition, we think there are dependencies on noise and display bit depth. We showed that effective noise could be much less than 1/10th of measured noise by doing noise filtering and image/video averaging. For display bit depth, a typical display bit depth for HMD is 8-bit that is 256-level. In order to show 1e- signal on HMD properly, there are on-going research efforts to improve image quality by doing the proper dark frame subtraction & black level control, noise filtering, tone mapping, and even with deep learning [2]. Figure 12 shows tone mapping examples in the HWK1411.

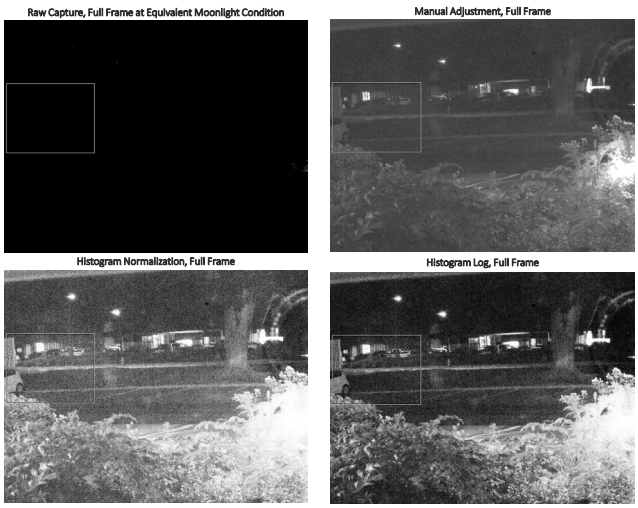

Figure 12. Tone mapping examples.

5. Conclusion

We presented the 9.5Mpixel HWK4123 and the 1.6Mpixel HWK1411 sensors with 0.5e- rms read noise implemented with 65nm sCMOS technology. These sensors are suitable for very low light imaging applications such as night vision. We have shown the sensor architectures, the analog signal path to achieve very low read noise, high near infrared quantum efficiency, and their performance. Based on these sensors, we present SNR measurements and sub-electron image and video processing results. The HWK1411 paves the way to achieve image and video capture down to overcast starlight condition, and enables transition of the night vision market to CMOS image sensors. This SWaP optimized design creates a forward-looking path to next-gen night vision systems to transform image system design at ultra-low-light conditions.

Acknowledgement

The authors gratefully acknowledge the contributions by HWK4123 and HWK1411 product design, product and test engineering, characterization and validation, hardware and software, and application engineering teams.

References

[1] Z. Shukri; "The-State-of-the-Art of CMOS Image Sensors", IISW, R01, 2021.

[2] J. Ma, et al.; "Review of Quanta Image Sensors for Ultralow-Light Imaging", IEEE Electron Devices, June 2022.